# EXPERIMENT 6 & 7: HARMONIC OSCILLATOR PART II. PHYSICAL PENDULUM AND WAVES ON A VIBRATING STRING

SAMUEL ELLISON – UID # 204977052

LAB PERFORMED ON 5/23/2018 AND 5/30/2018

LAB SECTION: WEDNESDAY 2PM

TA NAME: ERIK KRAMER

LAB PARTNERS: ERIC WONG AND MIKE MORIN

WORD COUNTS: ABSTRACT (199) BODY (3054)

# Analysis of Damped and Driven Physical Pendulum Oscillations and Behavior of Wave Motion on a Stretched String

*S. L. Ellison*[1]


## Abstract:

This report examines two separate phenomena: harmonic motion of a physical pendulum and standing waves on a stretched string. For the pendulum, I analyze under, over, critically damped, and driven motion to determine the undamped and resonance frequencies and the damping time, from which the Quality Factor is calculated. Constructing an Amplitude Spectrum with resonance width can provide an estimation for $Q$. Magnets and a wave driver damp and drive the pendulum's motion. Changing magnet spacing and driver frequency and analyzing various plots allowed me to determine all quantities. The resonance frequency $\omega_{\mathrm{R}} = 4.52 \pm 0.01\mathrm{rad/s}$ and damping time $\tau = 2.1 \pm 0.1\mathrm{s}$ produced $Q = 4.7 \pm 0.1$. The undamped frequency $\omega_0 = 4.41 \pm 0.02\mathrm{rad/s}$ and resonance width $\Delta\omega = 0.25 \pm 0.02\mathrm{rad/s}$ estimated $Q = 18 \pm 1$. For the stretched spring, the objective was to determine/compare predicted and measured wave speeds for different string tensions, and to predict, observe, and calculate normal modes and their frequencies by applying a vibration via a wave driver. Measured and predicted velocities with a string tension of $3.9511 \pm 0.0005\mathrm{N}$ were $26.11 \pm 0.04\mathrm{m/s}$ and $24.48 \pm 0.05\mathrm{m/s}$ respectively. A drive frequency of $8.163 \pm 0.002\mathrm{Hz}$ excited the fundamental mode. Higher modes $n$ had frequency of $n(8.163) \pm 0.002\mathrm{Hz}$. The predicted fundamental frequency was $8.326 \pm 0.007\mathrm{Hz}$. Applying a boundary decreased oscillation amplitude more when place at an antinode than at a node.


[1] *Department of Mechanical Engineering University of California Los Angeles*

**Introduction**

A physical pendulum is a rigid body that can rotate about an axis. Similar to a spring mass system, this pendulum will oscillate in simple harmonic motion if released from an initial displacement. Thus, the forces (in this case, torques) acting on the pendulum can be explained by a differential equation that, when solved, provides enough information to describe the exact motion. If a damping force and a driving force are added to the system, the physical pendulum may exhibit resonance. The purpose of this part of the experiment was to demonstrate undamped, underdamped, overdamped, critically damped, driven, and resonance pendulum oscillations while determining the angular frequencies, damping time, and ultimately, the Quality Factor associated with resonance. Damping magnets and a wave driver were applied to the system to demonstrate the different motions, and various plots were analyzed to determine relevant values. A stretched spring undergoing tension will exhibit standing wave patterns if vibrated at certain frequencies. The wave created by the string travels at a speed dependent on the strings tension and linear density. An observer will detect a standing wave if the string is vibrating with a frequency corresponding to a normal mode. The purpose of this part of the experiment was to measure and calculate wave speeds with different string tensions, determine frequencies corresponding to normal modes to exhibit standing waves, and to analyze the effect of boundary constraint places on the string on the Oscillation Amplitude. Hanging masses from a stretched string created different tensions, the wave driver induced vibrations, and a photodiode sensor could track the oscillatory motion of a point on the string.

**Methods**

First, I set up the pendulum system. I attached a PASCO Scientific Mechanical Vibrator (Wave Driver) to the top of a PASCO Stand and extended a clamp from the stand and attached and arranged the PASCO Scientific Rotation Sensor and the Metal, Anchor-Shaped Physical Pendulum so the pendulum could swing freely without touching the table. I attached a torsion spring from the wave driver to the pulley hole and set up a PASCO Photogate Sensor to standardize the starting position of the pendulum for all releases. I recorded Angle versus Time data for about 7 seconds after releasing the pendulum once with no damping magnets, and six times with damping magnets, each trial with different magnet spacing (10.0, 20.0, 30.0, 40.0, 50.0, and 13.8mm all with an uncertainty of $\pm 0.5$mm). I measured the spacing with a Starrett Meterstick. Next, I set the magnet gap to $40.0 \pm 0.5$mm and turned on the wave driver. After estimating what the resonance frequency was, I recorded Signal Generator versus Angle Data after releasing the pendulum for drive frequencies around this estimated frequency. It was determined the resonance frequency was $0.720 \pm 0.002$Hz because the Lissajous Figure for this frequency was most symmetric. I then recorded data for drive frequencies above ($0.780 \pm 0.002$Hz) and below ($0.650 \pm 0.002$Hz) the resonance frequency and observed the Lissajous Figures. Next, I recorded Angle versus Time data for the pendulum with drive frequencies of: 0.600, 0.650, 0.700, 0.710, 0.720, 0.730, 0.740, 0.770, 0.800, and 0.850 Hz all with an uncertainty of $\pm 0.002$Hz. After measuring the Amplitude of Oscillation from the Angle versus Time plot for each of these 10 frequencies, I plotted Amplitude (Normalized) versus Drive Frequency to create a Lorentzian curve.

First, I massed and measured the unstretched length of the string using an OHAUS Dial-O-Gram Balance and a Starrett Meter Stick. Then, I clamped one end of the string and measured the excess length and ran the other end over a PASCO super pulley. I set up the PASCO Scientific Mechanical Vibrator (Wave Driver) under the string at the clamped end and the PASCO Diode Laser and PASCO Light Sensor at the pulley end. I adjusted the laser, so it just covers the top of the string, and the sensor so it is directly above the part of the string with the laser. I connected all sensors to the DAQ. I hung masses of 250.00g, 350.00g, and 400.00g (all with an uncertainty of $\pm 0.05$g) from the pulley end and recorded the length of the string from the mass to the pulley for each case. I recorded the length of the stretched string from the pulley to the clamp. For each mass, I recorded Photodiode Signal versus Time plots after turning on the wave driver with a frequency of 0.250Hz and Amplitude 1V. With the $400.00 \pm 0.05$g mass attached, I observed Lissajous Figures of parametric plots of Light Intensity versus Output Voltage for wave driver frequencies ranging from about 8.000Hz to 42.000Hz (uncertainty $\pm 0.002$Hz) and determined which frequencies produced symmetric plots to conclude the normal mode frequencies 1 through 5. Then I constrained the string using another clamp in the center ($n = 2$ central node) and recorded data for frequencies corresponding to modes 2, 4, and 5.

## Analysis

### Damped and Driven Physical Pendulum Oscillations

The equations of motion for a damped physical pendulum is derived by summing all applied Torques:

$$\tau_{\text{grav}} \approx -MgL\theta, \tau_{\text{spring}} \approx -B\theta, \tau_{\text{damp}} = -b\dot{\theta}$$

$I\ddot{\theta} = -k\theta - b\dot{\theta}$ where $k = MgL + B$ and $I$ is the moment of inertia. (Equation 6.2[1])

Solving differential equation defines undamped and damped frequencies $\omega_0$ and $\omega_{\text{damp}}$, and damping time $\tau$:

$\theta(t) = Ae^{i\omega_{\text{damp}}t}e^{-t/\tau}$ (Eq. 6.4[1]) where $\omega_{\text{damp}} \equiv \sqrt{\frac{k}{I} - \frac{b^2}{4I^2}}$ (Eq. 6.5[1]), $\tau \equiv \frac{2I}{b}$ (Eq. 6.6[1]), and $\omega_0 \equiv \sqrt{\frac{k}{I}}$

Therefore, $\omega_{\text{damp}} \equiv \sqrt{\omega_0^2 - \frac{1}{\tau^2}}$. This allows us to define three regimes of damped motion:

Underdamped: $\omega_0 > \frac{1}{\tau}$ ($\omega_{\text{damp}}$ has all real solutions)

Overdamped: $\omega_0 < \frac{1}{\tau}$ ($\omega_{\text{damp}}$ has all imaginary solutions)

Critically Damped: $\omega_0 = \frac{1}{\tau}$ ($\omega_{\text{damp}} = 0$, the system returns to equilibrium state the fastest)

If we add a driving force to damped motion, a new term is added to the differential equation:
$I\ddot{\theta} = -k\theta - b\dot{\theta} + C\cos(\omega_{\text{d}}t)$ (Eq. 6.7[1]) where $\omega_{\text{d}}$ is the drive frequency. The resonance frequency $\omega_{\text{R}}$ is the maximum value of $\omega_{\text{d}}$ in the equation for $\theta(t)$. If the differential equation is solved, differentiated, set equal to 0, and solved for $\omega_{\text{d}}$, we obtain an equation for the resonance frequency:

$$\omega_{\text{R}} = \sqrt{\omega_0^2 - 2\frac{1}{\tau^2}} \text{ (Eq. 6.12[1]) where } Q \equiv \frac{1}{2}\tau\omega_{\text{R}} \text{ (Eq. 6.13[1])}$$

$Q$ is the Quality Factor of the damped driven oscillation. For cases where there is very low damping, the Quality Factor can also be approximated from $\omega_0$ and the width of the resonance curve $\Delta\omega$:

$$Q \approx \frac{\omega_0}{\Delta\omega} \text{ (Eq. 6.16[1])}$$

Note: The wave driver frequencies are cyclic frequencies $f$ (Hz) while the pendulum frequencies are angular frequencies $\omega$ (rad/s). These values are related by: $\omega = 2\pi f = 2\pi/T$ where $T$ is the period of oscillation.

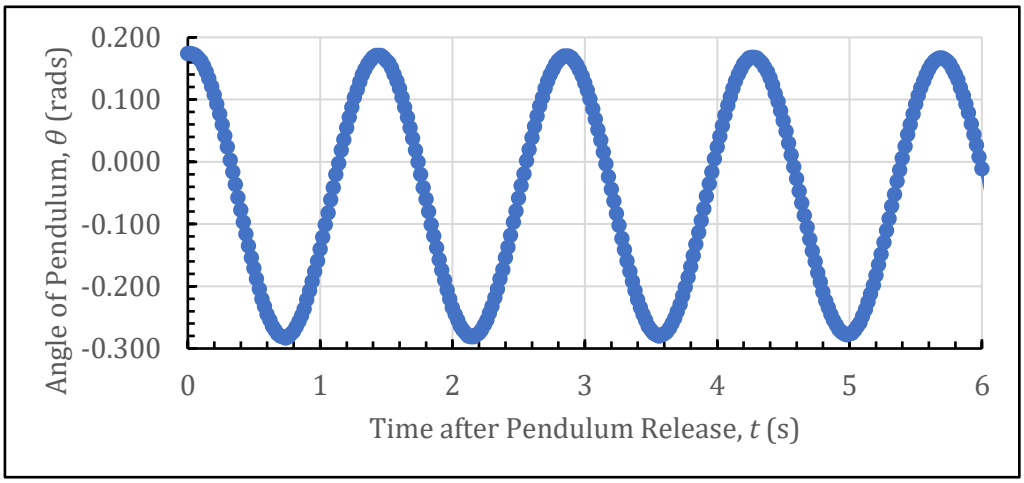


**Figure 1: Undamped, Undriven Motion of a Physical Pendulum.** The pendulum was tilted back to an initial angle $\theta$ and released, and the rotation sensor collected raw data (blue points) of the pendulum's angle over time. The period $T$ of this undamped motion is the time difference between peaks. Taking an average of the four $T$ values in the plot and using Eq. ii.13[1] to calculate uncertainty, we find $T = (1.425 \pm 0.005\text{s})$. The undamped frequency is $2\pi$ over the period: $\omega_0 = 4.41 \pm 0.02\text{rad/s}$. The uncertainty is propagated using Equation ii.25.[1]

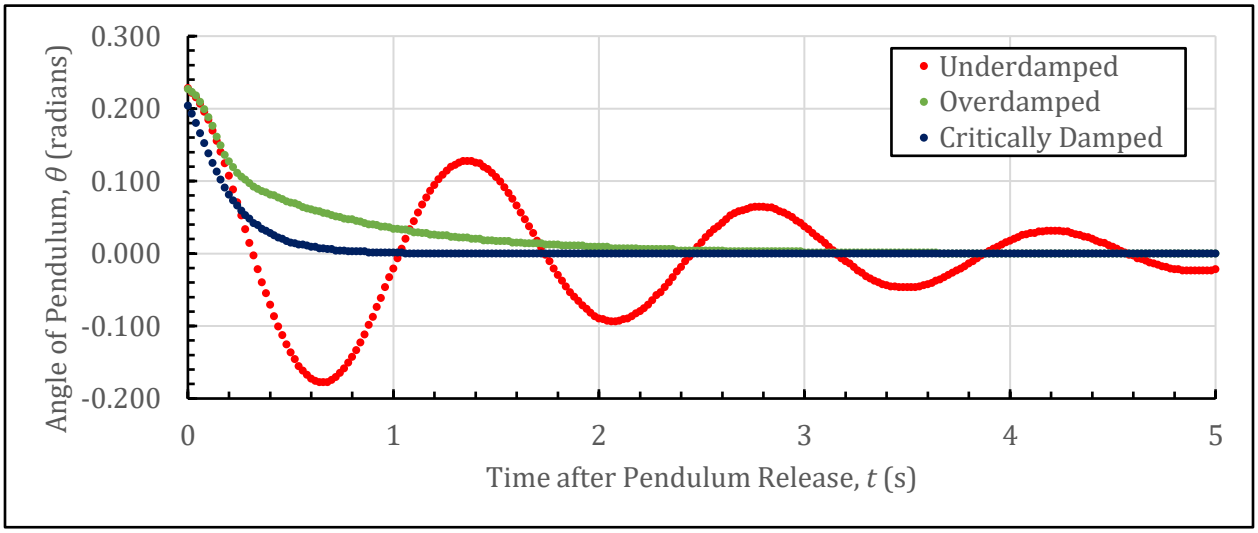


**Figure 2: Under, Over, and Critically Damped Motion of a Physical Pendulum.** The pendulum was extended and released through the same initial θ as with undamped, except two damping magnets were placed so the pendulum swings between them, damping its motion. The distance between the magnets determines how damped the motion will be. The red points represent a magnet separation of $30.0 \pm 0.5$mm corresponding to underdamped motion. The green points represent a magnet separation of $10.0 \pm 0.5$mm corresponding to overdamped motion. The blue points represent a magnet separation of $13.8 \pm 0.5$mm corresponding to critically damped motion. Note that the critically damped motion occurred when the pendulum reached an angle $\theta = 0$ the fastest.

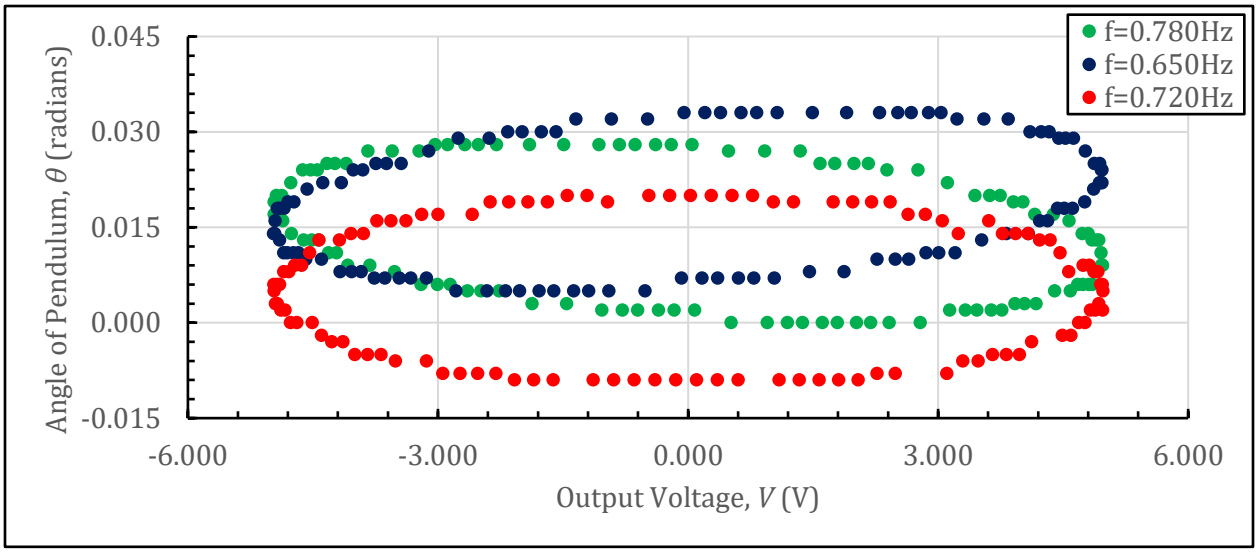


**Figure 3: Lissajous Figures (Parametric Plots) for Drive Frequencies Below, Above, and Right on Resonance.** The pendulum was again released from the same angle, but now underwent underdamped (magnet separation of $30.0 \pm 0.5$mm) *and* driven motion. Three different cyclic drive frequencies were applied to the system (seen in legend) and the angle vs the wave driver's output voltage was plotted (values are translated to show shapes). The error in cyclic frequency is $\delta f = 0.002$Hz because changing it by this value will just start to affect the shape of the plots. The blue and green data points are the raw data collected from a frequency below and above the resonance frequency (asymmetric Lissajous figures), respectively, and the red data were collected at resonance frequency (symmetric Lissajous figure). To determine the true angular resonance frequency $\omega_R$, I multiplied the cyclic frequency of the red data by $2\pi$ to get $\omega_R = 4.52 \pm 0.01$rad/s.

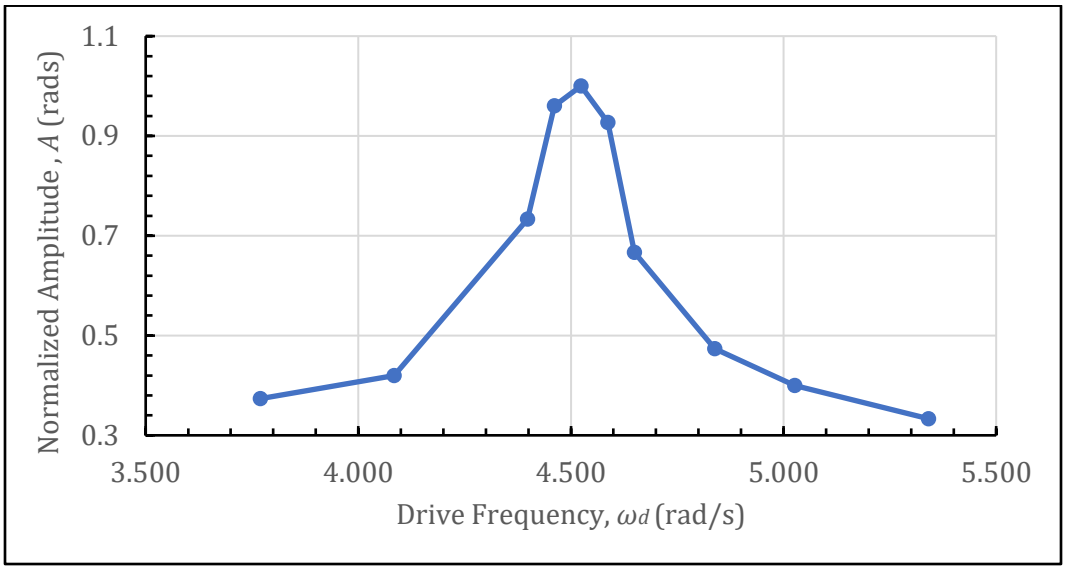


**Figure 4: Amplitude Spectrum for Various Drive Frequencies Applied to Physical Pendulum During Oscillation.** Various cyclic drive frequencies between 0.600 Hz and 0.850 Hz were applied to the pendulum via wave driver. Plots of Angle vs Time were analyzed to determine the Amplitude of Oscillation $A$ corresponding to each drive frequency. These Amplitudes are normalized to where the maximum Amplitude (located at $f = 0.720\text{Hz}$ or $\omega_R = 4.52 \pm 0.01\text{rad/s}$) is equal to 1. The blue points are the raw data corresponding to Normalized Amplitudes associated with various angular drive frequencies (converted from cyclic frequencies). The blue line connecting all points shows the Lorentzian shape of the plot. The width of the peak at $A = 1/\sqrt{2}$ rads represents the value for $\Delta\omega$. I concluded $\Delta\omega \approx 0.25 \pm 0.02\text{rad/s}$.

$\Delta\omega$ is a difference of drive frequencies, $\omega_{\text{d1}}$ and $\omega_{\text{d2}}$. Eq. ii.22 can apply to derive uncertainty:
$\Delta\omega = \omega_{\text{d1}} - \omega_{\text{d2}}$: $\delta(\Delta\omega) = \sqrt{(\omega_{\text{d1}})^2 + (\omega_{\text{d2}})^2}$. We know $\delta\omega_{\text{d}} = 2\pi(\delta f)$ so $\delta\omega_{\text{d1}}$ and $\delta\omega_{\text{d2}}$ are both ±0.01rad/s.

Therefore, $\delta(\Delta\omega) = \pm 0.02\text{rad/s}$

The damping time $\tau$ can be determined from the red curve in Figure 2: underdamped pendulum motion. $\tau$ is the time it takes the amplitude to decrease by a factor of $e$. Therefore:
$\tau = -\frac{T}{\ln[\frac{\theta(t+T)}{\theta(t)}]}$ where $T$ is the period, and $\frac{\theta(t+T)}{\theta(t)}$ is the ratio of consecutive peak amplitudes.
Using the four peaks in the red curve in Figure 2, three values of $\tau$ can be determined, and an average can be taken to find $\tau_{\text{best}}$. Uncertainty derived from Equation ii.13.[1] Therefore, $\tau = 2.1 \pm 0.1$ seconds. The Lissajous Figures of Figure 3 show that $\omega_{\text{R}} = 4.52 \pm 0.01\text{rad/s}$. Now that values for $\tau$ and $\omega_{\text{R}}$ have been determined, we can use Equation 6.13[1] to find $Q$:

$$Q \equiv \frac{1}{2}\tau\omega_{\text{R}} = 4.7 \pm 0.1 \text{ where } \delta Q = \frac{1}{2}Q\sqrt{(\frac{\delta\tau}{\tau})^2 + (\frac{\delta\omega_{\text{R}}}{\omega_{\text{R}}})^2}$$

An additional method to determine $Q$ is to analyze an Amplitude Spectrum of different drive frequencies. See Figure 4 above. Using the undamped frequency $\omega_0$ from Figure 1 and the Amplitude Spectrum width $\Delta\omega$, we can apply Equation 6.16:[1]

$$Q \approx \frac{\omega_0}{\Delta\omega} = 18 \pm 1 \text{ where } \delta Q = Q\sqrt{(\frac{\delta\Delta\omega}{\Delta\omega})^2 + (\frac{\delta\omega_0}{\omega_0})^2}$$

These two $Q$ values are extremely different. It is more difficult to trust the second method in calculating the Quality factor because the Lorentzian shape is an approximation, meaning $\Delta\omega$ will not have a very precise value, thus resulting in a large uncertainty for $Q$.

**Waves on a Vibrating String**

Values independent of Hanging Mass:

Total Length of Unstretched String: $L_T = 2.5125 \pm 0.0005\text{m}$
Excess String Length after Clamp: $L_{ex} = 0.5510 \pm 0.0005\text{m}$
Length of Vibrating String: $L = 1.5680 \pm 0.0005\text{m}$
Total Mass of String: $M_T = 0.01730 \pm 0.00005\text{kg}$

Three different masses ($m_1$) were hung from the end of the string. This resulted in different lengths of string hanging from the pulley ($L_1$). The mass of this part of the string ($m_2$), therefore, also contributes to the Tension in the part of the string undergoing vibration. So $T = (m_1 + m_2)g$. The linear mass density ($\mu$) of the vibrating string is given by the mass of only the vibrating string ($M$) divided by the length of the stretched string from the clamp to the mass ($L + L_1$). So $\mu = M/(L + L_1)$. Note: $m_2 = \mu L_1$, so the Tension can be written as $T = (m_1 + \mu L_1)g$.

The mass $M$ is calculated using Eq. 7.2:[1] $M = M_T\left(\frac{L_T - L_{ex}}{L_T}\right) = 0.01351 \pm 0.00005\text{kg}$

The predicted velocity is given by Eq. 7.1:[1] $v_p = \sqrt{\frac{T}{\mu}}$

| Hanging Mass, $m_1$ (kg) | Hanging String Length, $L_1$ (m) | Tension, $T$ (N) | Linear Mass Density, $\mu$ (kg/m) | Predicted Velocity, $v_p$ (m/s) |
|---|---|---|---|---|
| 0.25000±0.00005 | 0.4280±0.0005m | 2.4784±0.0005 | 0.00677±0.00003 | 19.14±0.04 |
| 0.35000±0.00005 | 0.4695±0.0005m | 3.4605±0.0005 | 0.00663±0.00003 | 22.84±0.05 |
| 0.40000±0.00005 | 0.4815±0.0005m | 3.9511±0.0005 | 0.00659±0.00003 | 24.48±0.05 |

**Table 1: Values needed to determine Predicted Wave Speeds from Three Different Hanging Masses.** Uncertainty propagations for mass $M$, Tension, Linear Mass Density, and Velocity are derived below using Equations ii.21[1], ii.22[1], ii.23[1], and ii.24.[1]

$$M = \frac{M_T x}{L_T}, (x = L_T - L_{ex}): \delta M = M\sqrt{(\frac{\delta M_T}{M_T})^2 + (\frac{\delta L_T}{L_T})^2 + (\frac{\delta x}{x})^2} = M\sqrt{(\frac{\delta M_T}{M_T})^2 + (\frac{\delta L_T}{L_T})^2 + (\frac{(\delta L_T)^2 + (\delta L_{ex})^2}{(L_T + L_{ex})^2})}$$

$$\mu = \frac{M}{x}, (x = L + L_1): \delta\mu = \mu\sqrt{(\frac{\delta M}{M})^2 + (\frac{\delta x}{x})^2} = \mu\sqrt{(\frac{\delta M}{M})^2 + (\frac{(\delta L)^2 + (\delta L_1)^2}{(L + L_1)^2})}$$

$$T = (m_1 + x)g = gy, (x = \mu L_1, y = m_1 + x): \delta T = g\delta y = \sqrt{(\delta m_1)^2 + (\mu L_1)^2\left[\left(\frac{\delta\mu}{\mu}\right)^2 + \left(\frac{\delta L_1}{L_1}\right)^2\right]}$$

$$v_p = (x)^{1/2}, (x = \frac{T}{\mu}): \delta v_p = \frac{1}{2}v_p\frac{\delta x}{x} = \frac{1}{2}v_p\sqrt{\left(\frac{\delta\mu}{\mu}\right)^2 + \left(\frac{\delta T}{T}\right)^2}$$

The definition of velocity is distance over time. Therefore, we can obtain a measured velocity using: $v_m = 2L/\Delta t$, where $\Delta t$ is the time it takes for the wave to travel $2L$. See Figures 5, 6, and 7 for determining $\Delta t$ values. The value for $2L = 3.136 \pm 0.001\text{m}$. The uncertainty is propagated below using Equation ii.23:[1]

$$v_m = \frac{2L}{\Delta t}: \delta v_m = 2v_m\sqrt{(\frac{\delta L}{L})^2 + (\frac{\delta\Delta t}{\Delta t})^2}$$

| Hanging Mass, $m_1$ (kg) | Time Interval Between Peaks, $\Delta t$ (s) | Measured Velocity, $v_m$ (m/s) |
|---|---|---|
| 0.25000±0.00005 | 0.1533±0.0003 | 20.46±0.04 |
| 0.35000±0.00005 | 0.1285±0.0002 | 22.40±0.04 |
| 0.40000±0.00005 | 0.1195±0.0002 | 26.11±0.04 |

**Table 2: Time Interval and Measured Wave Speeds for Three Different Hanging Masses.** The Figure captions in Figures 5, 6, and 7 explain how to determine $\Delta t$ and its uncertainty.

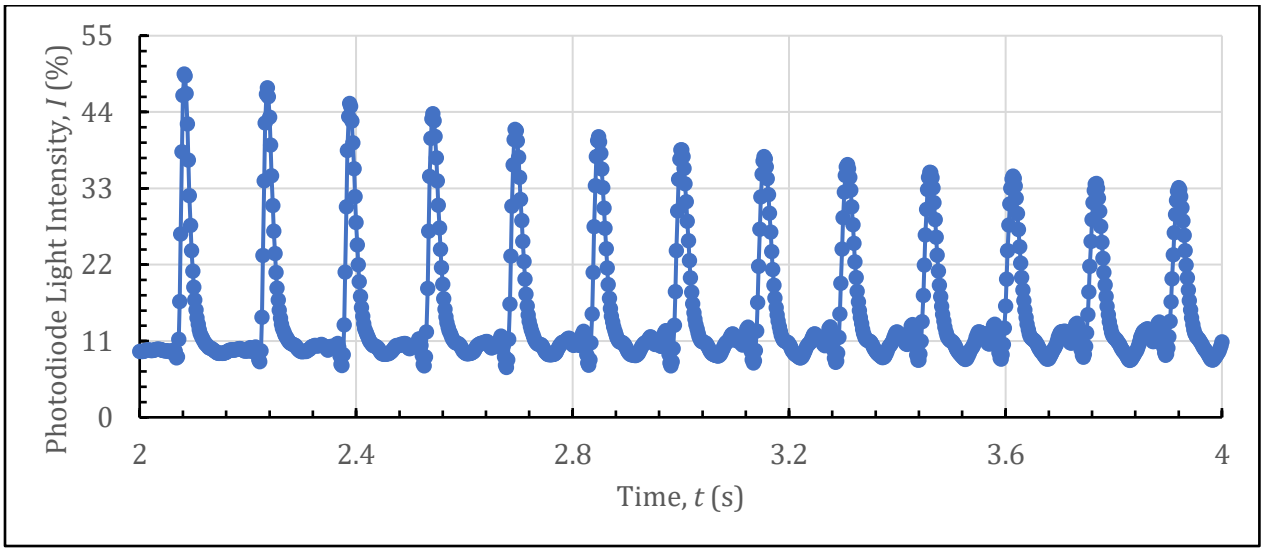


**Figure 5: Evaluating Wave Speed from Pulse Signal with String under 2.4784±0.0005N of Tension.** The wave driver was set to 0.250±0.002Hz and was turned on to vibrate the string (under 2.4784±0.0005N of Tension). The blue points are the raw data that the photodiode recorded (light intensity as a percentage) as a function of time. The blue line connects the points to show repeating features of the plot. The time interval $\Delta t$ between peaks represents the time it takes the wave to travel the distance of the vibrating string $L$ and back, or $2L$. Taking an average of all 12 $\Delta t$ values seen in the plot and using Eq. ii.13[1] to calculate uncertainty, we find $\Delta t = (0.1533 \pm 0.0003\text{s})$.

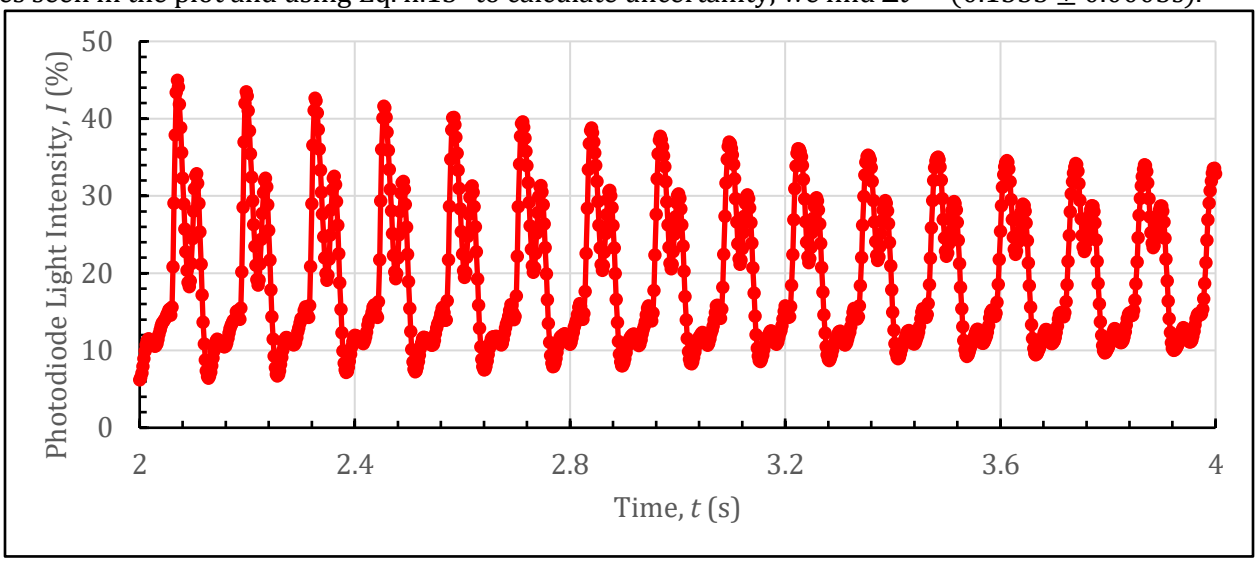


**Figure 6: Evaluating Wave Speed from Pulse Signal with String under 3.4605±0.0005N of Tension.** The same conditions as described in Figure 5, except the string was vibrating under 2.4784±0.0005N of Tension. Red points are the raw data taken from the photodiode and the red line connects the points to show repeating features. Using the same method to calculate the time interval, we find $\Delta t = (0.1285 \pm 0.0002\text{s})$.

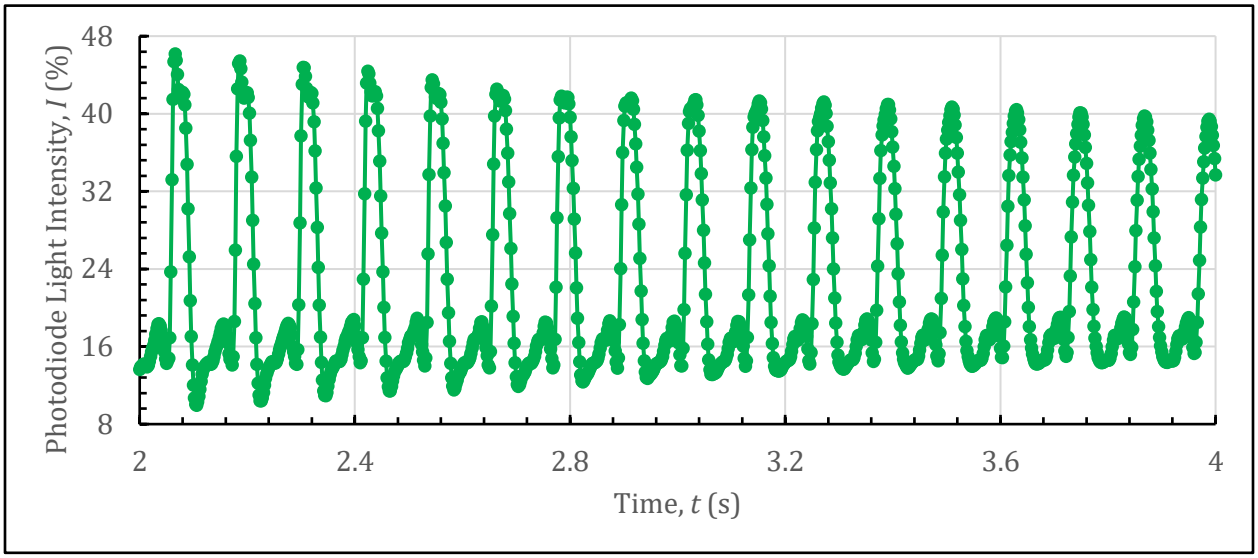


**Figure 7: Evaluating Wave Speed from Pulse Signal with String under $3.9511 \pm 0.0005$N of Tension.** The same conditions as described in Figure 5, except the string was vibrating under $3.9511 \pm 0.0005$N of Tension. Green points are the raw data taken from the photodiode and the green line connects the points to show repeating features. Using the same method to calculate the time interval, we find $\Delta t = (0.1195 \pm 0.0002s)$.

For all future trials, a hanging mass of 400.00±0.05g ($3.9511 \pm 0.0005$N of Tension) was hung from the string.

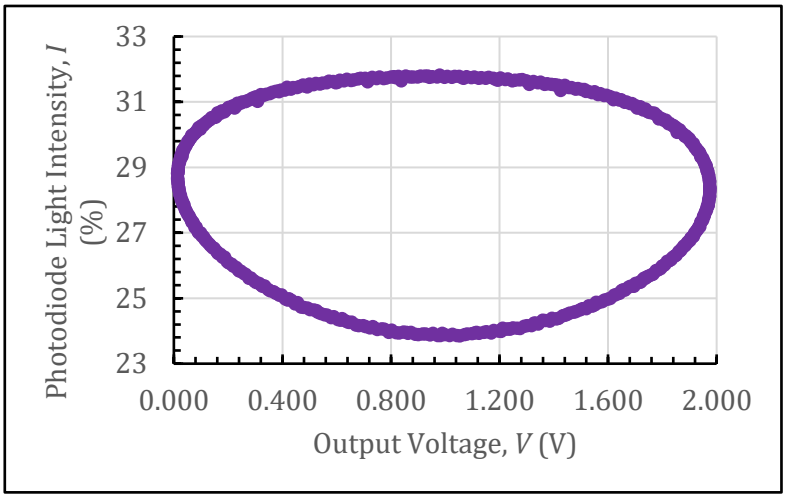


**Figure 8: Lissajous Figure (Parametric Plot) for Vibrating String under $3.9511 \pm 0.0005$N of Tension for the Fundamental Mode (n=1).** The wave driver was set to a frequency of $f = 8.163 \pm 0.002$Hz and vibrated the string which had a hanging mass of $400.00 \pm 0.05$g. The purple data points are the raw data for the parametric plot graphing Light Intensity and Output Voltage with a time parameter. The y-axis symmetry of this Lissajous Figure proves that this frequency does in fact excite a normal mode.

For higher order modes $n = 2, 3, 4, \& 5$, the wave driver was set to a frequency $f = n(8.163)$Hz, and it was observed that the Lissajous plots were symmetric, and the vibrating string demonstrated a normal mode. See Table 3 for values of these observed fundamental frequencies. To predict what these frequencies should be, we used Equation 7.3[1] where $v$ is the measured velocity for string with hanging mass 400.00±0.05g. See Table 2.

$$f = n\frac{v}{2L} \text{ where } \delta f = f\frac{n}{2}\sqrt{(\frac{\delta v}{v})^2 + (\frac{\delta L}{L})^2} \text{ (by Eq. ii.23[1])}$$

| Normal Mode, $n$ | Predicted Frequency, $f_p$ (Hz) | Observed Frequency, $f_{obs}$ (Hz) |
|---|---|---|
| 1 | 8.326±0.007 | 8.163±0.002 |
| 2 | 16.65±0.03 | 16.326±0.002 |
| 3 | 24.98±0.06 | 24.489±0.002 |
| 4 | 33.3±0.1 | 32.652±0.002 |
| 5 | 41.6±0.2 | 40.815±0.002 |
| 30 | 250±50 | |

**Table 3: Correspondence Between Predicted and Observed Standing Wave Velocities for Normal Modes $n = 1$ through 5 and 30.** The n=30 mode was not observed. The uncertainty in observed frequency propagated from the wave driver sensitivity and determined to be ±0.002Hz.

| Normal Mode, $n$ | Photodiode Amplitude Without Constraint, $A$ (%) | Photodiode Amplitude With Constraint, $A_C$ (%) |
|---|---|---|
| 2 | 5.520 ± 0.006 | 0.163±0.007 |
| 4 | 2.59±0.02 | 0.19±0.02 |
| 5 | 2.18±0.03 | 0.017±0.002 |

**Table 4: Effect of a Central Boundary Constraint on Normal Mode Photodiode Amplitudes:** Frequencies corresponding to normal modes 2, 4, and 5 were applied to the string with and without a constraint clamp in the center of the string. Photodiode Light Intensity versus Time graphs were plotted. The average amplitude was determined (uncertainty from Eq. ii.13[1]) from all plots and recorded in this table. Note that the constraint reduced the Photodiode Amplitude more in the case in which the clamp was placed at an antinode (n=5) than when placed at a node (n=4 and n=2).

## Conclusion

The goal of the two experiments was to one, determine the Quality Factor of a physical pendulum's damped, driven oscillation through two different methods using undamped and resonance frequencies, damping time, and resonance width, and then comparing the values. Two, to calculate and compare predicted and measured velocities of a vibrating string (under various Tensions) and frequencies of normal modes (under the same Tension), and then observe the effect of a central constraint on the standing wave Amplitude. For the physical pendulum, the undamped frequency was $\omega_0 = 4.41 \pm 0.02$rad/s (from Figure 1), the resonance frequency was $\omega_R = 4.52 \pm 0.01$rad/s (from Lissajous Figures of Figure 3), the damping time was $\tau = 2.1 \pm 0.1$ seconds (From underdamped oscillation of Figure 3), the resonance width was $\Delta\omega \approx 0.250 \pm 0.02$rad/s (from Lorentzian shape of Figure 4). The calculated Q-factor from damping time and resonance frequency was $Q = 4.7 \pm 0.1$ and the estimated Q-factor from undamped frequency and resonance width was $Q = 18 \pm 1$. These two Q values are significantly different; however, we concluded that the estimated value is not as trustworthy because the resonance width is an imprecise quantity resulting in $Q$'s large uncertainty. Using Eq. 7.1,[1] the predicted velocities for the vibrating string with hanging masses of 250.00g, 350.00g, and 400.00g (all with uncertainty ±0.05g) were 19.14±0.04m/s, 22.84±0.05m/s, and 24.48±0.05m/s respectively. Using the definition of velocity and the Pulse Signal Plots (Figures 5, 6, and 7), the measured velocities for those hanging masses were 20.46±0.04m/s, 22.40±0.04m/s, and 26.11±0.04m/s. Overall, measured velocities are greater, but both demonstrate that greater Tension produces greater wave speed. The observed frequencies that excited normal modes $n = 1$ through 5 on the string had values of $n(8.163) \pm 0.002$Hz while the predicted fundamental frequency was $8.326 \pm 0.007$Hz. The frequencies are similar, yet they do not overlap with uncertainties. A central boundary constraint clearly reduced oscillation amplitude more when placed at an antinode than node (n=5 compared to n=2,4). A systematic uncertainty arises from string. Because of the string's mass and thickness, gravity has an influence on individual particles' oscillations along the vibrating string. Thus, the wave speed is damped by the force of gravity. To improve this, A thinner, lighter string should be used, and operating in a vacuum would eliminate air resistance.

References

[1] Campbell, W.C. *et al*. Physics 4AL: Mechanics Lab Manual (ver. April 3, 2017). (University of California Los Angeles, Los Angeles, California).